Chemical Geology 278 (2010) 70–79

Contents lists available at ScienceDirect

Chemical Geology

journal homepage: www.elsevier.com/locate/chemgeo

Research paper

The determination of labile Fe in ferrihydrite by ascorbic acid extraction: Methodology, dissolution kinetics and loss of solubility with age and de-watering

Rob Raiswell *, Hong Phuc Vu, Loredana Brinza, Liane G. Benning

School of Earth and Environment, Leeds University, Leeds LS2 9JT, UK

ARTICLE INFO

Article history:
Received 11 February 2010
Received in revised form 23 August 2010
Accepted 1 September 2010

Editor: J.D. Blum

Keywords:
Ferrihydrite
Ascorbic acid
Dissolution kinetics
Aggregation
Aging

ABSTRACT

An ascorbic acid extraction at pH 7.5 has been examined to assess the influence of reaction conditions (pH, ascorbic acid concentration) on the dissolution of Fe from synthetic 2-line ferrihydrite and from other Fe-bearing minerals. The method was highly selective for Fe in ferrihydrite with only small amounts of Fe extracted from other (oxyhydr)oxides or clays. The labile Fe extracted from the synthetic 2-line ferrihydrite stored as a slurry decreased with time, and high resolution microscopy showed that the older materials formed networked aggregates that slow down the dissolution. The apparent rate constant for the dissolution of fresh 2-line ferrihydrite ($\sim 10^{-3}\ s^{-1}$) was an order of magnitude larger than that for aged suspensions ($\sim 10^{-4}\ s^{-1}$). Fresh 2-line ferrihydrite that was filtered, freeze-dried, frozen and freeze-dried, and stored in the dry was even less readily dissolved (apparent rate constants $\sim 10^{-6}\ s^{-1}$). These ferrihydrites also contained networked aggregates and, additionally, appear to occur as granular aggregates (visible to the naked eye) during the early stages of dissolution. Storage of filtered, freeze-dried, and frozen and freeze-dried ferrihydrites, whether in water or air, produced similar dissolution behaviour because aggregation caused by de-watering decreases the labile Fe content and is not reversed by re-hydration. The determination of labile Fe in ferrihydrite requires that natural samples should be collected, stored and extracted wet. The most aged samples dissolved by parabolic dissolution kinetics indicate that the rates of dissolution were controlled by the diffusion of reactant into the internal porosity of aggregates.

© 2010 Elsevier B.V. All rights reserved.

1. Introduction

The delivery of particulate Fe as (oxyhydr)oxides to the ocean exerts an important influence on the levels of dissolved, bioavailable Fe (Moffett, 2001), especially in Fe-limited regions such as the Southern Ocean (Raiswell et al., 2006, 2008a,b). Unfortunately it is difficult to define the bioavailability of Fe (oxyhydr)oxides due to the variations in their mineralogy, grain-sizes and crystallinity. Furthermore the extraction of bioavailable Fe from potential mineral sources can occur by a variety of mechanisms, including dissolution, photochemical reactions, grazing and direct ingestion (Wells and Mayer, 1991; Johnson et al., 1994; Barbeau et al., 1996; Yoshida et al., 2002). No simple chemical extraction can replicate the diversity of these processes, nevertheless extractions are commonly used to determine labile or bioavailable Fe because of their speed and simplicity (e.g. Wells et al., 1991; Chen and Siefert, 2003; Berger et al., 2008).

However, culture experiments (Wells et al., 1983; Rich and Morel, 1990; Wells et al., 1991; Nodwell and Price, 2001) have shown that only 2-line ferrihydrite (often described as amorphous hydrous ferric oxide, HFO or $Fe(OH)_3$) can support diatom growth, but even this relatively labile (oxyhydr)oxide may only become bioavailable following photochemical reduction or grazing (Wells and Mayer, 1991; Johnson et al., 1994; Barbeau et al., 1996). These experiments utilised synthetic HFO whereas Visser et al. (2003) utilised soil dusts that contained natural aged and dried HFO that contained only 20–30% labile Fe that was soluble in seawater (see later discussion). Increases in diatom growth were positively correlated with the amount of HFO but dissolved Fe was not completely available for the diatoms. Yoshida et al. (2002) have also shown that Fe can be solubilised by marine siderophores from HFO (and possibly also goethite) at seawater pH. Clearly a chemical extraction which selectively dissolves labile Fe from ferrihydrite would be an important tool to facilitate studies of potentially bioavailable particulate Fe.

The most widely used chemical extractions for Fe are those utilising dithionite (Mehra and Jackson, 1960; Canfield, 1989), hydroxylamine hydrochloride (Chester and Hughes, 1967; Berger et al. 2008) or ammonium oxalate (McKeague and Day, 1966; Philips and Lovely, 1987). Comparisons between these methods (Kostka and Luther, 1994; Raiswell et al., 1994; Poulton and Canfield, 2005) have clearly shown that hydroxylamine hydrochloride is the most selective for ferrihydrite, yet even this extraction quantitatively dissolved lepidocrocite and also extracted significant amounts of Fe from magnetite and chlorite.

* Corresponding author. Tel.: +44 1133 435200; fax: +44 1133 435259.
E-mail address: r.raiswell@see.leeds.ac.uk (R. Raiswell).

0009-2541/$ – see front matter © 2010 Elsevier B.V. All rights reserved.
doi:10.1016/j.chemgeo.2010.09.002

However, the studies by Ferdelman (1988), Kostka and Luther (1994), Reyes and Torrent (1997) and Hyacinthe and Van Cappellen (2004) indicate that Fe may be extracted from ferrihydrite with a high degree of selectivity by an ascorbic acid–sodium citrate–sodium bicarbonate mixture. Kostka and Luther (1994) showed that a 24 h extraction at pH 8 with shaking at room temperature achieves the quantitative dissolution of fresh ferrihydrite without removing any Fe from goethite, hematite, magnetite and chlorite. Hyacinthe and Van Cappellen (2004) used slightly more acid conditions (pH 7.5) to show that this extraction dissolves varying proportions of ferrihydrite depending on crystallinity, aging and drying (>97% of fresh 6-line nano-ferrihydrite, 75–97% of aged 6-line nano-ferrihydrite, 25–50% aged and freeze-dried 6-line nano-ferrihydrite, 75–97% of fresh amorphous HFO, and 3–25% aged and freeze-dried 2-line nano-ferrihydrite). Since all ferrihydrite is nanoparticulate (Janney et al. 2000, 2001), the 'nano' prefix is subsequently only used where appropriate for other Fe minerals. With more refractory iron minerals, Hyacinthe and Van Cappellen (2004) showed that the extraction efficiency for lepidocrocite, and fresh nano-hematite was 25–50%, while the equivalent freeze-dried nano-hematite was only weakly extracted (3–25%). Furthermore crystalline hematite was essentially unreactive (<3% extracted), but no extraction efficiencies were reported for other iron minerals at this pH. These data clearly show that the Fe from ferrihydrite was more readily extracted than from other Fe (oxyhydr)oxides but that the efficiency of extraction varied with aging and sample treatment both of which affected the amount of nanoparticulate Fe mineral that was extracted.

Fe oxyhydr(oxide) nanoparticles are known to undergo aggregation in suspension and when the water is removed by drying or freeze-drying (Waychunas, 2001; Gilbert et al., 2007), both of which have a significant effect on aggregate morphology, particularly the interior structure and porosity (Cornell and Schwertmann, 2003; Gilbert et al., 2009). Gilbert et al. (2009) showed that aggregation of Fe oxyhydr(oxide) nanoparticles produced more compact structures with lower internal porosity which decreased the uptake of metals. De-watering was particularly effective at decreasing the capacity for metal uptake (Bottero et al., 1993; Scheinost et al., 2001) which Gilbert et al. (2009) concluded was due to loss of surface area plus an increasing difficulty in transporting ions into the interior porosity of more compacted, aggregated structures. Nurmi et al. (2005) and Cwiertny et al. (2009) have also emphasized that aggregation may play an important role in determining the reactivity of iron (oxyhydr) oxide nanoparticulates. These findings provide a possible explanation for the variability in extraction efficiencies observed by Hyacinthe and Van Cappellen (2004) for ferrihydrites dried and aged in different ways, because more compact and aggregated structures will inhibit access of the relatively large ascorbate ion into the interior porosity.

To address this issue, we have evaluated the performance of the ascorbic acid extraction at pH 7.5 over a range of reaction conditions and sample treatments in order to establish a reliable methodology appropriate for measuring labile and potentially bioavailable Fe in small samples such as iceberg sediment and atmospheric dust (Raiswell et al., 2008a,b; Shi et al., 2009, in press), that can also be applied to small samples from other settings (e.g., filtered samples from deep sea vents and seawater particulates). Visser et al. (2003) found that the Fe extracted by ascorbic acid from the HFO in soil dust, and that which was dissolved from the dust in seawater, were able to increase the growth rate of diatoms, although these sources were not completely bioavailable. However Hyacinthe et al. (2006) have shown that 65% of the Fe extracted by this technique is microbially bioavailable. The ascorbic acid extraction was the preferred choice on the basis of selectivity (see previous discussion) and because the reaction mechanism is well-established (Banwart et al., 1989; Sulzberger et al., 1989; Dos Santos et al., 1990). There have also been valuable kinetic studies by Postma (1993) and Larsen and Postma (2001) who have provided a quantitative framework to compare the effects of sample treatment on Fe extraction. Thus the aims of this study were: (1) to optimise the extraction conditions and assess their selectivity in relation to typical iron-bearing minerals found in sediments, specifically glacial sediments and atmospheric dust and (2) to examine the effects of aging and sample treatment on synthetic 2-line ferrihydrites by studying the dissolution kinetics of Fe in ascorbic acid.

2. Experimental conditions

2.1. Extraction procedures

The extraction conditions were optimised using a freeze-dried 2-line ferrihydrite (F) that was approximately 6 months old (and was thus relatively stable with respect to further aging; see later discussion). In a first set of experiments the effects of different extraction conditions were evaluated. Sub-samples of the ferrihydrite F were treated for 24 h by an ascorbic acid solution buffered at pH 7.5. The extractant was a deoxygenated solution of 50 g L^{-1} sodium citrate (0.17 M) and 50 g L^{-1} sodium bicarbonate (0.6 M) to which 10 g L^{-1} of ascorbic acid (0.057 M) was added. About 30 mg of the sample was mixed with 10 mL of the ascorbic acid mixture, shaken for 24 h at room temperature and then filtered through 0.45 μm membrane filters and the aqueous fraction was analysed for Fe (see later discussion). The labile Fe dissolved by ascorbic acid is hereafter termed FeA. In order to test the effect of pH (see later discussion) on this extraction procedure, sub-samples of ferrihydrite F were reacted with ascorbic acid with the pH adjusted to range from 7.0 to 8.5. Extractions were also carried out at ascorbic acid concentrations varying from 0.057 to 0.17 M.

In a second set of experiments the selectivity of the ascorbic acid extraction was evaluated. Extractions were carried out sequentially using the ascorbic acid technique described earlier followed by a dithionite extraction (see Raiswell et al., 1994). This sequential procedure was tested on a range of iron (oxyhydr)oxides (lepidocrocite, hematite, goethite, and magnetite, Poulton and Canfield, 2005), two samples of schwertmannite (a ferric (oxy)hydroxyl-sulfate; see Raiswell et al., 2009), and three standard clays. The standard clays were supplied from the Special Clays section of the Clay Mineral Repository and consisted of an illite (Silver Hill, Montana, USA), an illite/smectite (Czechoslovakia) and a smectite (Crook, Wyoming, USA). In the dithionite procedure, the materials remaining after the extraction by ascorbic acid were treated for 2 h with a solution of 50 g L^{-1} sodium dithionite in 0.35 M acetic acid and 0.2 M sodium citrate, buffered at pH 4.8 (see Raiswell et al., 1994). Dithionite-soluble Fe is hereafter termed FeD. Both FeA and FeD extractant solutions were analysed for Fe by atomic absorption spectrophotometry with an air-acetylene flame.

2.2. Kinetic studies

The kinetic experiments were carried out on freshly prepared ferrihydrite and a suite of ferrihydrites that had been de-watered, stored and aged in different ways. Fresh 2-line ferrihydrite was synthesized (Cornell and Schwertmann, 2003) by dissolving 40 g of Fe $(NO_3)_3\ 9H_2O$ in 500 mL deionized water to which 300 mL of 1 M NaOH were quickly added with constant stirring to raise the pH to ~7.0. The final volumes of NaOH were added carefully to avoid overshooting the pH. After precipitation the ferrihydrite was centrifuged and washed at least 4 times to ensure that the resulting slurry (hereafter termed FS) was free of electrolyte residue. The density was determined from the weight loss of a known amount of slurry (in triplicate) after drying at 50 °C for 24 h. These densities were used to calculate the amount of FS utilised in the dissolution experiments (0.1 g of ferrihydrite was contained in 1.282 g of slurry).

A portion of this fresh ferrihydrite (FS) was retained as the original slurry and stored at room temperature at a pH of 6–6.5. Different portions of this slurry (Fig. 1) were de-watered by suction filtering

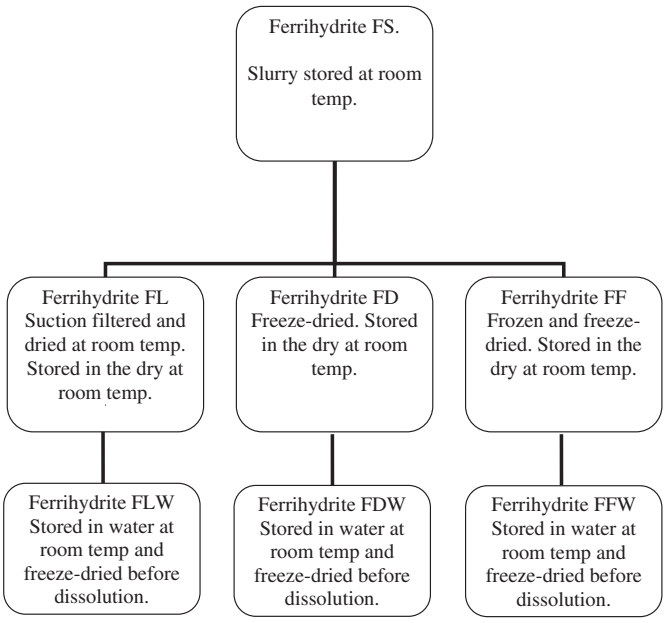

Fig. 1. Ferrihydrite samples and storage treatments.

(FL), freeze-drying (FD) and freezing and freeze-drying (FF). FL was de-watered by filtering through a 0.45 μm filter, allowed to air dry and then gently disaggregated with a pestle and mortar. FF was frozen overnight at −20 °C, then thawed and the supernatant removed by pipetting before the remaining material was freeze-dried. Finally, FD was freeze-dried overnight using a standard lyophilyzer (E.C. Modulyu). Each of the resulting materials was stored in the dry at room temperature. In addition, 0.5–1 g sub-samples of FL, FD and FF were each stored in 100 mL water (which evolved to a final pH of ~4) at room temperature. These sub-samples were used for kinetic studies by removing a portion of the solids, each of which was then freeze-dried (respectively termed FLW, FDW and FFW). All seven samples were examined by X-ray diffraction and high resolution microscopy to determine the changes in mineralogy and/or morphology during storage and/or reaction with ascorbic acid.

Kinetic studies on these ferrihydrites were carried out by reacting ~0.1 g of sample in 500 mL of a continuously stirred ascorbic acid solution (prepared as described earlier). The supernatant was sampled at regular intervals over periods of time of 1–2 h (for FS) to up to 50–100 h (for the other ferrihydrites) by removing a sample of the extractant from just below the solution surface to minimize loss of ferrihydrite. Samples of FS were filtered through 0.2 μm membrane filters and samples of FL, FD, FF, FLW, FDW and FFW were filtered through 0.45 μm membrane filters. Fe analysis was carried out as described earlier.

Fresh and aged samples of each ferrihydrite type were characterized before and after extraction by conventional X-ray powder diffraction using a Philips PW1050 X-ray diffractometer operating at 40 kV and 30 mA with a CuKα radiation. Samples were loaded onto silicon sample holders and diffraction patterns were collected over the 2θ range between 5 and 70° with a rate scan of 0.08°/min (for 14 h) and step size of 0.01. This produced detailed high resolution scans such that even small proportions of crystalline materials could be detected (see later discussion).

The morphology and aggregate structure of the ferrihydrites were characterized using a high resolution Field Emission Gun Scanning Electron Microscope (FEG-SEM, LEO 1530 system). Dried samples were ground gently in an agate mortar, dispersed in 100% ethanol solution in an ultrasonic bath and pipetted onto an Al-sample stub. The samples were dried, coated with a 5 nm Pt layer using an Agar high resolution sputter coater with a Pt source and imaged at 3 keV and a working distance of 3 mm.

The crystal size, structure, crystallinity and high resolution characteristics of all ferrihydrites were investigated by Field Emission Gun Transmission Electron Microscopy (CM200 FEG TEM) operating at 197 kV. The minerals were dispersed in methanol using an ultrasonic bath and then pipetted onto an Agar standard holey carbon support film. Energy dispersive spectra (EDS) and selected area electron diffraction (SAED) patterns were collected in order to assess the elemental contents and to determine the *d* spacings for the studied materials. These were then compared with bulk diffraction patterns from the conventional XRD analyses of the same samples and standard values from literature.

The BET surface areas of the fresh and aged ferrihydrites were measured using a Gemini V2365 system (Micromeritics Instrument Corp.). Prior to analysis, all samples were freeze-dried, weighed and de-gassed with nitrogen at 22 °C for at least 16 h. BET measurements were performed using N_2 as the adsorbate with 11 points of analysis, relative pressure from 0.05 to 0.3, evacuation rate of 300 mm Hg/min, an optimum pressure of 760 mm Hg and an equilibration time of 10 s.

3. Results and interpretation

3.1. Morphology, mineralogy and surface area

High resolution SEM, TEM and XRD data presented in Figs. 2 and 3 show the morphology and mineralogy of the ferrihydrites in their freshly prepared state and after aging for 85–125 days. Fresh FS comprised only 2-line ferrihydrite (identified by the XRD pattern in Fig. 2a) mainly present as networks of large coalesced aggregates (up to 20–300 nm diameter), which were in turn made up of smaller nanoparticle aggregates (Fig. 2b). The higher resolution TEM image of the same sample (Fig. 2c) shows that the ferrihydrite (confirmed by the two diffuse rings in the SAED pattern, Fig. 2c inset) occurred as poorly crystalline nanoparticles (~5 nm diameter). Microphotographs of freshly prepared FF (Fig. 2d), FD and FL displayed the same nanoscale characteristics but at a macro-scale drying has compacted the aggregates. Upon aging as a slurry for 85–125 days the FS sample consisted of rounded aggregates but these now appear more compacted and networked (Fig. 3b, compare with Fig. 2b). We will term this phenomena as network aggregation. Conventional powder XRD revealed the presence of small amounts of goethite and hematite but the two broad hump representatives of 2-line ferrihydrite are still visible (Fig.3a). In addition, the presence of goethite and hematite was confirmed by TEM through their characteristic morphologies and SAED patterns (Fig. 3c). Aged samples of FF, FL and FD (Fig. 3d–f) also show the development of compacted networked aggregates (compare to Fig. 2d). However, in contrast to the aged FS sample, slow scan XRD revealed 2-line ferrihydrite as the sole phase in the FF, FL and FD samples (both fresh and aged in the dry for 130–140 days). Surface area measurements for the ferrihydrites showed small increases (outside our analytical error) in the surface area after 24 h treatment with ascorbic acid (FF 224 to 247 $m^2\ g^{-1}$; FL 151 to 200 $m^2\ g^{-1}$ and FD 190 to 208 $m^2\ g^{-1}$).

3.2. Optimising extraction conditions

Extraction proceeds by reductive dissolution using ascorbic acid with citrate acting as a chelating agent. Banwart et al. (1989) have observed that the rate of dissolution of hematite increased with ascorbic acid concentration up to 0.5 mM (~1 g L^{-1}) at which point there is more than enough ascorbate to be adsorbed to the surface. The surface areas of our ferrihydrites are 150–230 $m^2\ g^{-1}$, approximately 10-fold higher than the hematite used by Banwart et al. (1989). However, there was no change in the extraction of Fe from the 2-line ferrihydrite F (Table 1) for ascorbic acid concentrations up to 30 g L^{-1} (0.17 M). Note that ferrihydrite F had a total Fe content of

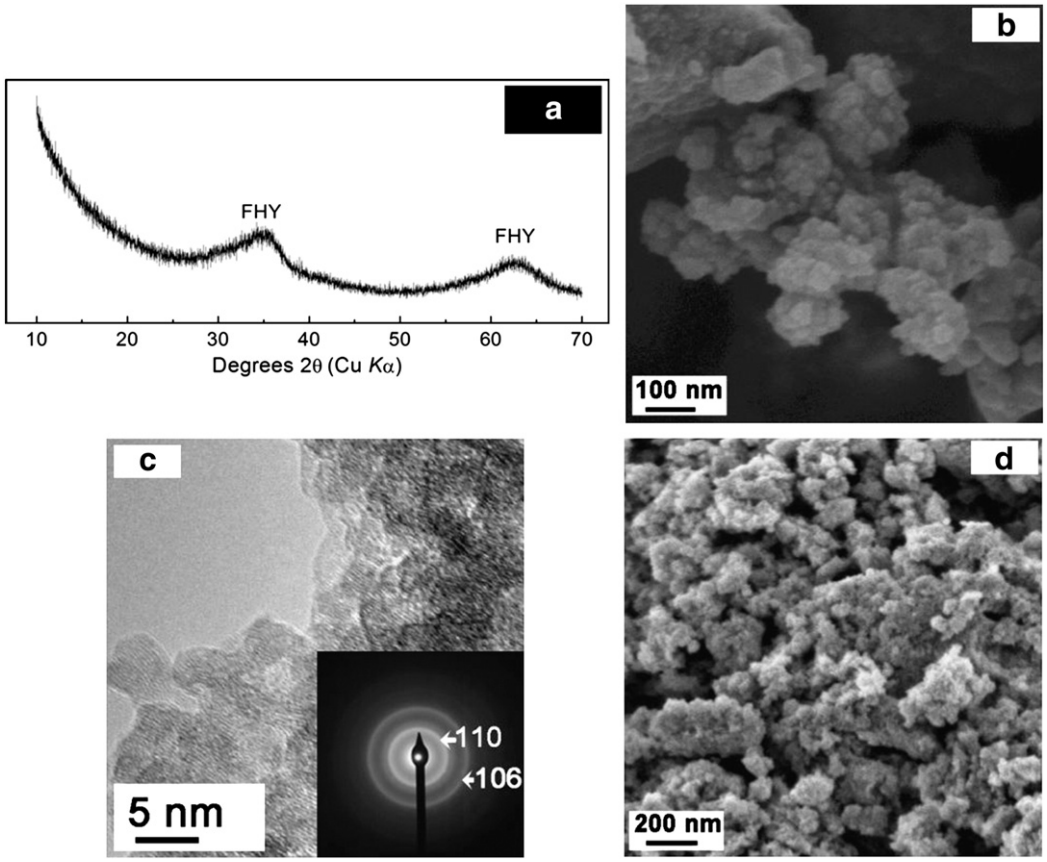

Fig. 2. (a) Slow scan XRD of fresh ferrihydrite FS. (b) SEM microphotograph of fresh ferrihydrite FS. (c) TEM of fresh ferrihydrite FS, with inset of corresponding Bragg reflections. (d) SEM microphotograph of fresh ferrihydrite FF (characteristic ferrihydrite lines shown by FHY).

53.8% but only 9.98% FeA was extracted from this 6 month old material (see later discussion).

The aforementioned extractions were carried out at pH 7.5 but the dissolution mechanism involves the adsorption of the electroactive ascorbate ion (HA^-) the concentration of which varies with pH and Dos Santos et al. (1990) give;

$$[HA^-] = [H_2A] / \left(1 + \left[H^+\right] / K_a\right)$$

where $K_a = 9.1 \times 10^{-5}$ for ascorbic acid. With $[H_2A]$ concentrations of ~0.06 M and pH = 7.5 the term $[H^+]/K_a \ll 1$ and small changes in pH have no effect on $[HA^-]$. However, Dos Santos et al. (1990) state that the pH does affect the extraction of magnetite because the density of reactive sites increases 3-fold as the pH decreases from 8 to 7.5. No equivalent data exist for ferrihydrite and extractions were therefore carried out on the ferrihydrite F with the pH adjusted by addition of ascorbic acid to range from 7.0 to 8.5.

These data (Table 2) gave a linear trend such that;

$$\%Fe = 39.5 - 4.3\ pH \quad (r = 0.99)$$

hence a pH change of 0.1 produced a change of 0.8% Fe, equivalent to a 10% error at pH 7.5. Careful control of pH is needed to avoid errors that exceed the analytical precision.

3.3. Selectivity and precision

Table 3 reports the results from the sequential extractions using ascorbic acid (% FeA) followed by dithionite (% FeD) on iron (oxyhydr) oxides, iron (oxy)hydroxy sulfates and clay standards. The (oxyhydr) oxide results are comparable to those reported by Hyacinthe and Van Cappellen (2004) at pH 7.5 in that only fresh 2-line ferrihydrite (FS) was quantitatively extracted. Our freeze-dried and aged 2-line ferrihydrite was partially extracted (9.98% FeA) as was freeze-dried and aged 6-line ferrihydrite (4.0% FeA). Schwertmannite and As-rich schwertmannite were also partially extracted (12.4% and 8.4% FeA respectively) but negligible amounts of FeA were extracted from lepidocrocite, hematite, goethite and magnetite. Table 3 also shows that clay minerals only supplied very small concentrations of ascorbic acid-soluble Fe. The residual Fe in all the oxyhydr(oxide) minerals, except magnetite, was however substantially dissolved by dithionite (% FeD in Table 3), consistent with Raiswell et al. (1994) and Poulton and Canfield (2005). There are no natural materials for which there are recommended values for ascorbic acid-extractable Fe and hence accuracy on natural ferrihydrites is difficult to estimate. Precision was estimated from replicate analyses of the aged, freeze-dried, 2-line ferrihydrite F (9.98% FeA, precision ~8%) and a glacial sediment (0.109% FeA; precision ~8%).

3.4. Dissolution kinetics

Different de-watering treatments and aging may affect extraction by causing aggregation which reduces the accessibility of reagents to the aggregate interior (Gilbert et al., 2009). We have explored the effects of aging and de-watering on 2-line ferrihydrite (prepared and treated in different ways) using the kinetic framework developed by Postma (1993). This approach is based on a method from Christoffersen and Christoffersen (1976) for analysing data from dissolution experiments where there are large variations in the sizes and number of crystals. Postma (1993) showed that the following general rate law can be defined:

$$J = k\ t\ m_o\ F(m / m_o) S(C) \quad (1)$$

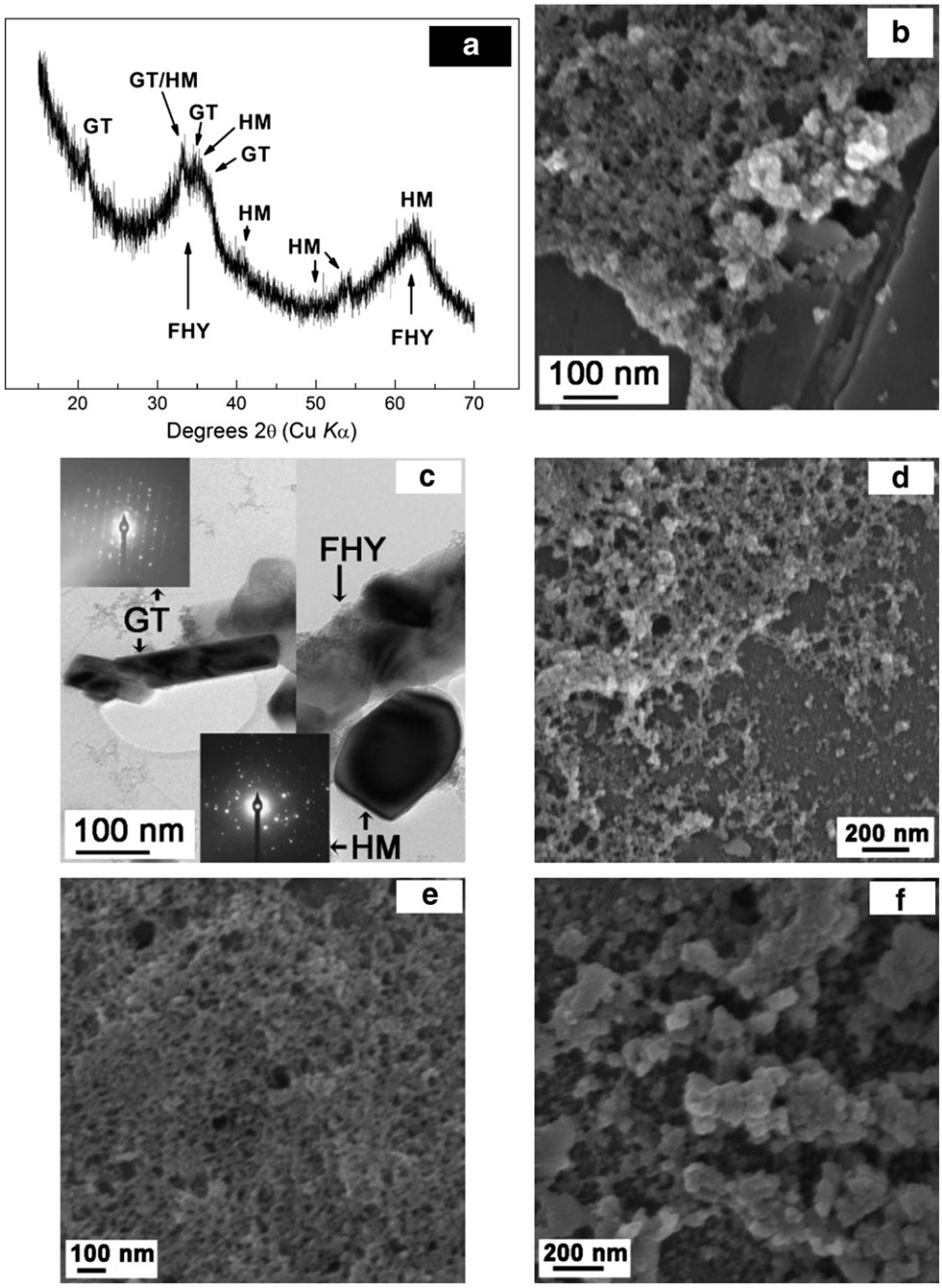

Fig. 3. (a) Slow scan XRD of aged (85 days old) ferrihydrite FS showing characteristic lines of ferrihydrite FHY, goethite GT and hematite HM. (b) SEM microphotograph of the same aged ferrihydrite FS. (c) TEM of aged FS showing the presence of goethite and hematite with inset of corresponding Bragg reflections. (d, e, f) SEM microphotographs of aged (85 days) ferrihydrites FF, FL and FD respectively showing networks and aggregates of small ferrihydrite particles. No goethite or hematite was identified by slow scan XRD or high resolution TEM in these samples.

where J = the overall rate of dissolution (mol s^{-1}), m_o = the initial mass of crystals (mol), m = the mass of crystals (mol) remaining after time t (s) and k = the rate constant (s^{-1}). The term $F(m/m_o)$ is a function of changes in crystal size, morphology, reactive site density, etc. during dissolution and is usually expressed as the function $(m/m_o)^{\gamma}$, where γ depends on (surface area)/(mass), grain-size distribution and

Table 1
Variation in Fe dissolved at pH 7.5 from aged 2-line ferrihydrite F as a function of ascorbic acid concentration.

Ascorbic acid conc g L^{-1}(M)	% FeA
10 (0.057 M)	9.4 ± 0.8
17.5 (0.1 M)	10.5 ± 0.8
20 (0.11 M)	9.2 ± 0.8
30 (0.17 M)	10.8 ± 0.8

Table 2
Variation in Fe dissolved from aged 2-line ferrihydrite F by 0.057 M ascorbic acid at different pH.

Extraction pH	% FeA
8.45	3.8 ± 0.3
8.00	5.1 ± 0.4
7.55	7.4 ± 0.6
7.02	9.7 ± 0.8

Table 3
Iron dissolved sequentially by ascorbic acid (% FeA) and dithionite (% FeD) compared to the total Fe content for common Fe-bearing minerals.

Mineral	% FeA	% FeD	% Total Fe
Fresh 2-line ferrihydrite FS[a]	53.8	–	53.8
Aged 2-line ferrihydrite F[a]	9.98	44.0	54.0
Freeze-dried and aged 6-line ferrihydrite[a]	4.0	47.4	51.4
Schwertmannite[a]	12.2	30.0	42.2
As-rich schwertmannite[a]	8.4	28.5	43.0
Lepidocrocite[b]	0.42	54.0	62.8
Hematite[b]	0.004	23.5	69.8
Goethite[b]	0.03	42.4	62.8
Magnetite[b]	0.09	5.44	72.3
Illite[c]	0.051	0.41	5.60
Illite/smectite[c]	0.024	0.26	0.80
Smectite[c]	0.031	0.21	2.60

[a] Total Fe is % FeA + % FeD. Schwertmannite data from Raiswell et al. (2009).
[b] Total Fe from Poulton and Canfield (2005).
[c] Data from Zongbo Shi (in prep.).

reactive site density (Larsen and Postma, 2001). The term S (C) is a function of the solution composition, such as the type and concentration of the reactant and is considered constant for ascorbic acid dissolution under the conditions used here (Postma, 1993). Larsen and Postma (2001) showed that for constant S (C) Eq. (1) simplifies to:

$$J/m_o = k'(m/m_o)^{\gamma} \quad (2)$$

where the apparent rate constant $k' = k\,S(C)$. Larsen and Postma (2001) plotted Eq. (2) in a logarithmic form:

$$\log(J/m_o) = \gamma \log(m/m_o) + k' \quad (3)$$

that provides straight lines with slope γ and intercept k'. Eq. (3) provides a useful way of comparing the dissolution behaviour (γ) and dissolution rate constants (k') for the seven ferrihydrites (FS, FL, FD, FF, FLW, FDW and FFW).

3.4.1. Ferrihydrite FS

Kinetic studies of this ferrihydrite slurry were carried out on fresh material (3 days after precipitation) and on slurries aged at room temperature for up to 126 days after precipitation (Fig. 4). The materials aged for 3 and 11 days gave good straight line plots for log (J/m_o) against log (m/m_o), with slopes giving $\gamma = 0.75$ and 0.45 and intercepts giving $k' = 10.3\times10^{-4}$ and $4.1\times10^{-4}\,s^{-1}$ respectively (see Supplementary content Table S1). The linear trends defined by Eq. (3) indicate that γ, and hence $F(m/m_o)$, remains constant and thus the distribution of crystal sizes, morphologies and reactive site densities remains constant as the material is lost by dissolution. The dissolution rate J/m_o is initially high but declines as m/m_o declines due to the loss of material by dissolution.

The older materials gave non-linear trends for Eq. (3) indicating that changes in crystal size, morphology and/or reactive site density occurred during dissolution (Fig. 4). The 56, 85 and 126 day old materials showed complex trends in log (J/m_o) which pass through a minimum (after 3–4 h) before increasing towards erratic plateau values. None of these data could be sensibly resolved into straight lines that allowed k' and γ to be determined. However, the later data points tend towards plateau values of log (J/m_o) which were extrapolated back through the dissolution minima to log (m/m_o) = 0 (on the y axis) to provide an estimate of the apparent rate constant k'. These estimates are only semi-quantitative because not all experiments reached plateau values. Nevertheless, used with caution and interpreted in conjunction with the data plots, these k' values allow rates of dissolution to be compared by removing the early changes in crystal size, morphology and/or reactive site density. Each k' value was roughly estimated from the mean and standard deviation of J/m_o values for the last 4 points in each experiment (where there is limited variation in J/m_o with changing m/m_o). These estimates of k' were compared with the k' values derived from the straight line plots of the 3 day and 11 day aged material (Fig. 4 and see Supplementary content Table S1). The apparent rate constant decreased by an order of magnitude as the FS slurry was stored at room temperature for 126 days and the data follow a power law (Fig. 5)

$$k' = 0.001(\text{Time in days})^{-0.6}$$

which suggests that k' approaches an assymptotic value of $\sim 10^{-4}\,s^{-1}$ after 50–100 days.

3.4.2. Ferrihydrites FL, FD and FF

Kinetic studies of these ferrihydrites were carried on material stored dry for 3–7 days, and up to 139 days, after preparation from FS. There were some notable differences in the behaviour of FL, FF and FD, as compared to FS, on their immersion in ascorbic acid. The FL, FF and FD materials, particularly the older materials, often remained as discrete granules (instead of becoming dispersed) for several hours after immersion during which there were pronounced minima in the plots of log (J/m_o) against log (m/m_o). Hereafter we refer to materials showing this behaviour as granular aggregates.

The resulting erratic trends for these samples (see Supplementary content, Fig. S1A–D) in the plots of log (J/m_o) against log (m/m_o) prevent the determination of k' and γ, as was the case with the older FS samples (see earlier discussion). However, apparent rate constants for these samples were derived as for the older FS samples by averaging the last four data points where log (J/m_o) remained roughly constant. These apparent rate constants are shown in Table 5. All three ferrihydrites were dissolved approximately three orders of magnitude more slowly

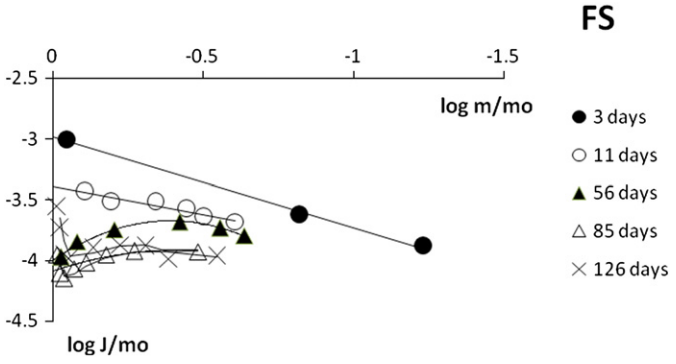

Fig. 4. Variations in ferrihydrite FS dissolution rates (J) normalised to initial mass (m_o) as a function of the proportion (m/m_o) of the solid phase remaining for aged FS (after Postma, 1993).

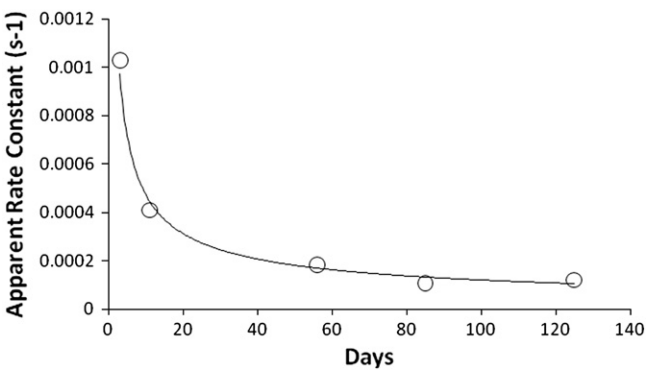

Fig. 5. Variation in the apparent rate constant (k') for the dissolution of ferrihydrite FS with storage time. Best fit curve describes $k' = 0.001\ (\text{days})^{-0.6}$.

than the FS from which they were prepared; k′ for the 3 day old FS is 10^{-3} s^{-1} (Fig. 5) but k′ for the 3–7 day old FL, FF and FD is ~10^{-6} s^{-1} (Table 4). Visser et al. (2003) found that the HFO fraction of aged and dried soil dust had comparable rate constants of ~10^{-6} s^{-1}. Clearly de-watering produces substantial decreases in the rates of dissolution.

The apparent rate constants of the ferrihydrites decreased in the order FL>FF = FD. Both FL and FF appear to show decreases in k′ with time (Table 4) but age trends were difficult to isolate from dispersion effects where the dissolution minima are prolonged and plateau values may not be reached. The age trend for FL was more certain than that for FF because the decrease from the 3–7 day old material to the 139 day old material was larger, and because the 139 day old FL was closer to a plateau value (compare Supplementary content Fig. S1A and S1B). It is possible that the more readily soluble FL which has higher initial k′ (4.7×10^{-6} as compared to 1.3×10^{-6} s^{-1} for FF) has the greater capacity for further decreases in the rate of dissolution.

3.4.3. Ferrihydrites FLW, FDW and FFW

Kinetic studies of these ferrihydrites were carried on a material that had been stored at room temperature in water (which evolved to a final pH~4) and then freeze-dried when required for dissolution. These materials all gave erratic trends for log (J/m_o) against log (m/m_o) (see Supplementary content Fig. S2A–C) often with dissolution minima associated with the slow dispersion of granular aggregates. Most of the data reached well-defined plateau values except for the 153 day old FLW and the 58 day old FFW data and apparent rate constants were derived as mentioned earlier from the later stages of dissolution (Table 5).

These data show that storage in water (with subsequent freeze-drying) apparently had little effect on dissolution rates compared to that of the precursor material. Thus the apparent rate constants of FL and FLW, FD and FDW and FF and FFW are essentially similar (compare the 3–7 day data in Table 4 with the 58 and 108–126 day data in Table 5). There was no clear evidence of changes in rates of dissolution with continued storage, since these changes would rely on the poorly-defined plateau values for the 153 day old FLW and the 58 day old FFW.

4. Synthesis

In general the kinetic studies of our ferrihydrites exhibited a range of aggregation and transformation effects due to aging and different storage conditions. We have observed the aggregation to produce coalesced nanoparticulates, networked aggregates (both observed at the microscopic level) and granular aggregates (observed at a macroscopic level). These effects are apparent at different scales but may be related (and may represent an age progression).

The kinetic data for FS showed two significant features (Fig. 4). First, changes in crystal size, morphology, reactive site density, etc. were absent during dissolution of the 3 and 11 day old samples but occurred during dissolution of the older materials; second, rates of dissolution generally decreased in the older materials. Both features are attributable to aggregation.

Table 4
Influence of de-watering and aging on the apparent rate constants (k′) for the dissolution of the ferrihydrites FL, FD and FF in 0.057 M ascorbic acid at pH 7.5.

Days after prep. from FS	FL. Apparent rate constant ($k'\times10^{-6}$ s^{-1})	FF. Apparent rate constant ($k'\times10^{-6}$ s^{-1})	FD. Apparent rate constant ($k'\times10^{-6}$ s^{-1})
3–7	4.7 ± 1.1	1.3 ± 0.1	0.6 ± 0.2[a]
52–56	1.9 ± 0.2	2.2 ± 0.2	1.5 ± 0.2
101–108	2.5 ± 0.3	1.2 ± 0.2	1.1 ± 0.2
139	0.9 ± 0.1	0.3 ± 0.03[a]	1.0 ± 0.2

[a] Plateau values may not have been reached.

Table 5
Influence of storage and aging on the apparent rate constants (k′) for the dissolution of the ferrihydrites FLW, FDW and FFW 0.057 M ascorbic acid at pH 7.5.

Days stored in water	FLW. Apparent rate constant ($k'\times10^{-6}$ s^{-1})	FFW. Apparent rate constant ($k'\times10^{-6}$ s^{-1})	FDW. Apparent rate constant ($k'\times10^{-6}$ s^{-1})
58	4.2 ± 0.7	0.9 ± 0.3[a]	0.4 ± 0.1
108–126	3.7 ± 1.2	1.9 ± 0.4	0.9 ± 0.2
153	0.7 ± 0.2[a]	2.5 ± 0.5	0.6 ± 0.1

[a] Plateau values may not have been reached.

The slopes of the plots of log (J/m_o) against log (m/m_o) for the fresh ferrihydrites produced values of k′ for 3 day and 11 day old FS which were 10.3×10^{-4} and 4.1×10^{-4} s^{-1} respectively. The rather lower values of 7.6 and 6.6×10^{-4} s^{-1} for the ferrihydrites of Larsen and Postma (2001) may have been affected by the presence of nano-hematite whereas high resolution microscopy and slow scan XRD of our 3 and 11 day old material only revealed 2-line ferrihydrite. The plots of Eq. (3) for our 3 and 11 day old FS material produced γ values of 0.75 and 0.45. Values of 0.67 are typical for isometric crystals such as cubes or spheres where the rate of dissolution depends only on the change in surface area as a function of decreasing mass. For example, Christoffersen et al. (1978) have found γ = 0.6 for the dissolution of rectangular hydroxyapatite crystals with approximately cubic cross-sections. Our γ data are thus consistent with the occurrence of freshly prepared ferrihydrites as rounded coalesced nanoparticulate aggregates (Fig. 2b) uncontaminated by, or not yet transformed to, goethite and hematite (see earlier discussion).

The non-linear dissolution behaviour of the older FS samples (Fig. 4) indicates that changes in crystal size, morphology, reactive site density etc. occurred during dissolution. These changes produced a decrease in the apparent rate constant of about an order of magnitude over 50–100 days (see earlier discussion). Rose and Waite (2003) observed a faster rate of aging for an HFO suspension in seawater at pH 8 which produced a decrease in the first order rate constant of about two orders of magnitude in one week. Decreases in rate of dissolution with aging have also been noted by Liu and Millero (2002) and Deng and Stumm (1994).

The dissolution minima in Fig. 4 for FS were not accompanied by the visually obvious discrete granules that were observed in the early dissolution behaviour of all the other ferrihydrites. Nevertheless dissolution minima occurred which suggest that aggregates, formed in the FS slurry, were breaking down and dispersing in ascorbic acid. Consistent with this, our microscopy data show that aging affected FS by producing more compact, networked aggregates (compare Figs. 2b and 3b). Nanoparticles typically undergo aggregation which affects their reactivity (Nurmi et al., 2005; Cwiertny et al., 2009) and Gilbert et al. (2007) observed that nanoclusters (25–1000 nm diameter) formed in a ferrihydrite suspension after several hours at pH 6. The formation of these nanoclusters was not reversible. Gilbert et al. (2009) observed changes in the interior structure and porosity of nanoparticulate aggregates which affected their ability to take up ions from solution (as required for dissolution). The existence of dissolution minima (Fig. 4) suggests that stirring may cause the looser network aggregates to break up (Logan and Kilps, 1995). Once these aggregates have been dispersed, the final stages of the dissolution and thus kinetic behaviour in Fig. 4 were a result of the dissolution of the residual material that contained coalesced aggregates and networked aggregates that were unaffected by stirring.

Besides aggregation effects, the transformation of the ferrihydrite to more crystalline iron phases was also initiated in the aged FS slurries (56–126 days old) which all contained small amounts of goethite and hematite (Fig. 3a and c), although ferrihydrite was still predominant in these samples (as indicated by the two broad humps in Fig. 3a). Schwertmann et al. (2004) estimated a half-life of ~100 days for the transformation of ferrihydrite to goethite/hematite

mixtures at 25 °C and our slurry pH (6–6.5). However, our FS slurry was stored at a higher solid/liquid ratio (~0.1) as compared to 0.01 for the materials studied by Schwertmann et al. (2004). Davidson et al. (2008) and Brinza (2010) have found that higher solid/liquid ratios (0.05 to 0.13) produce more aggregation and faster transformation, although they used higher temperatures or higher storage pH (7 to 8). Our FS samples only showed a limited transformation of ferrihydrite to goethite/hematite (see earlier discussion) which suggests that aggregation occurs more quickly than transformation at room temperature and a lower pH but high solid/liquid ratios.

The ferrihydrites FL, FF and FD were de-watered in different ways but stored in the dry. Transformation to goethite/hematite mixtures is extremely slow in the dry (Stanjek and Weidler, 1992) and, consistent with this, we observe no goethite or hematite in the slow scan XRD or microscopic analyses for these samples even after 139 days. Kinetic differences are thus solely attributable to aggregation, which we have observed to produce coalesced, networked and granular aggregates. The ferrihydrites FL, FF and FD all dissolved significantly less rapidly than the precursor FS from which they were prepared (Table 5). This is consistent with Gilbert et al. (2009) who have shown that aggregation by de-watering/drying is more effective than aggregation in solution. The former produces more compact nanoporous aggregates with a diminished capacity for ion adsorption (because transport into less porous aggregates is difficult). De-watering by filtering and air drying seems to produce the smallest decrease in the rate of dissolution, while the larger decreases for freezing and freeze-drying may arise because these treatments dehydrated the samples more effectively and hence encouraged more aggregation.

The 3–7 day old treated ferrihydrites (FL, FD, and FF) rapidly dispersed in ascorbic acid to produce a fine suspension. The older FL, FD and FF ferrihydrites (>52 days) differed from the younger materials in two ways. First, TEM and SEM images (Fig. 3b, d, e and f) showed that the aged materials were organised into network aggregates that were absent in the less aged materials (see Fig. 2d). Second, the older materials displayed macroscopic aggregation in the form of granular aggregates which survived for several hours in solution before dispersion (which was particularly slow for all the 139 day old FL, FF and FD materials). Aggregation could be accompanied by increased ordering that was undetectable by SAED, however the increase in the BET surface areas of FL, FD and FF after a 24 h treatment with ascorbic acid indicates that dissolution is accompanied by destruction of at least some aggregates. Our approach of defining k′ from near-plateau values in effect removes network and granular aggregation effects that produce the dissolution minima. However, once the granular aggregates have been dispersed the ferrihydrites FF and FD displayed no significant changes in the rate of dissolution with age (Table 4). By contrast FL, the most readily soluble of these ferrihydrites, does appear to dissolve less rapidly with increasing age. This was either because freezing and freeze-drying produced aggregates that were more difficult to breakdown or because this relatively soluble material could still be influenced by further aggregation or restructuring.

The materials FLW, FDW and FFW were separated from the 3 to 7 day old parent materials (FL, FD and FF), and stored in water for different lengths of time (Table 5). A portion of each product was de-watered by freeze-drying before the kinetic study. Storage in water for periods of time up to 153 days essentially produced no more than minor changes in the rate of dissolution except for FLW (as was also the case for FL). Aggregation effects that were induced by filtering, freezing and freeze-drying were thus unaltered during the storage and freeze-drying steps associated with separation of FLW from FL, FDW from FD and FFW from FF. Gilbert et al. (2009) concluded that aggregation is prevented by mutual repulsion when the pH is less than the pH_{ZPC} (typically ~7.8 for ferrihydrite but may decrease to ~6 due to adsorbed ions; Raiswell et al., 2006). Hence storage at pH 4 may have counteracted further aggregation.

The absence of any observable changes in the mineralogy of FLW, FFW and FDW during storage in water at pH~4 for 153 days was unexpected (Table 5). Schwertmann et al. (2004) estimate that the half-life for the conversion of ferrihydrite to goethite/hematite mixtures is approximately 200 days at this pH. We have not found goethite or hematite in these aged samples, perhaps because of differences in the storage conditions and/or sample treatments in our experiments compared to Schwertmann et al. (2004).

Table 5 shows no clear evidence of a decline in solubility over 153 days (except possibly for FLW) although these ferrihydrites appeared to change their kinetic behaviour. Fig. 6 shows that older FDW materials evolved towards parabolic dissolution kinetics (linear plots against the square root of time for ~100 h after a lag of 1 h). Parabolic kinetics are most obvious for the FLW and FDW ferrihydrites (Fig. 7) but the other ferrihydrites display near-linear relationships between Fe removed from the solid phase and the square root of time for a period of up to 100 h. Liang et al. (2000) also show data for the dissolution of ferrihydrite by citrate (at pH 6.5 for <100 h) and ascorbate (at pH 4 for <20 h) that display parabolic dissolution kinetics. Such relationships are typical of transport-controlled dissolution where diffusion through a leached layer limits the transfer of solvent into the solid phases and/or solute away from the solid. We interpret transport-controlled dissolution kinetics to indicate that aggregation limits the entry of the ascorbate ion into the intergranular porosity in these older, more aggregated materials. Aggregation effects that limit the entry of the ascorbate ion may also explain why increasing concentrations of ascorbic acid produced no corresponding increases in Fe extraction (Table 1).

Thus our data suggest that the decrease in rates of dissolution for ferrihydrites was due to a combination of two factors; rate of aggregation (whether forming coalesced, networked or granular aggregates) and rate of transformation to goethite/hematite mixtures (as summarised schematically in Fig. 8). The FS ferrihydrites stored as slurries undergo relatively rapid aggregation followed by gradual transformation and thus plot in the region of Fig. 8 where dissolution behaviour is controlled by both mineralogical changes and reactant/solute transport. Conversely all the ferrihydrites that were dried by filtering, freeze-drying or freezing (stored dry and in water) plot in the upper region of Fig. 8, where the rate of aggregation is faster than the rate of transformation. Aggregation in these ferrihydrites has occurred on both a microscopic and a macroscopic scale. The dissolution of ferrihydrites in this region is controlled more by transport than mineralogy, more evidently for FF, FFW, FD, FDW than FL and FLW.

5. Conclusions

The ascorbic acid extraction provides a simple and reliable measurement technique that is highly specific for the Fe present in

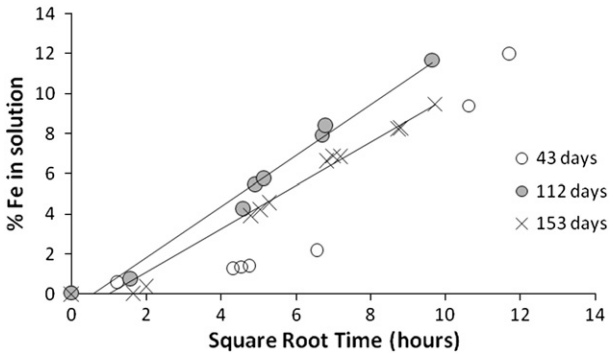

Fig. 6. Fe content of the ascorbic acid solution as a function of the square root of time (hours) for the dissolution of the ferrihydrite FDW. Note near-linearity of 112 and 153 day old samples.

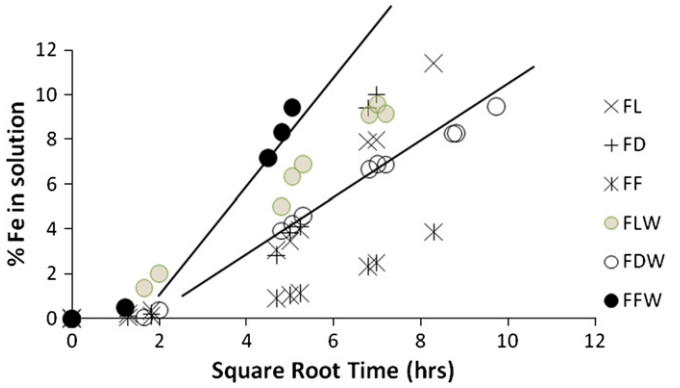

Fig. 7. Fe content of the ascorbic acid solution as a function of the square root of time (hours) for the dissolution of the most aged ferrihydrites FL, FD, FF, FLW, FDW and FFW. Lines denote an envelope of data that is near-linear.

fresh 2-line ferrihydrite. We have shown that the extraction efficiency of Fe from ferrihydrite (and thus the labile Fe content) declines with age and de-watering, mainly because of aggregation and, to a lesser extent, because of transformation to goethite and hematite. The extraction efficiency decreased with de-watering, but suction filtering (and subsequent air drying) showed smaller decreases in rates of dissolution as compared to freeze-drying and freezing (with subsequent freeze-drying). Benning et al. (2000) have found that freeze-drying iron monosulfide produced a decrease in reactivity (and surface area). We suggest that freezing (followed by freeze-drying) and freeze-drying alone are harsher treatments that produce greater aggregation which decreases the rate of dissolution of these materials. Our microscopy observations and kinetic data support the conclusions of Gilbert et al. (2009) that aggregation produces compact nanoporous aggregates with an interior porosity that is less accessible to dissolved species which decreases the rate of dissolution. Extreme aggregation produces dissolution behaviour that is transport-controlled because the nano-porosity limits entry of reactant and/or removal of solute.

Granular aggregation effects may be reversed by crushing but not by ultrasonication, although crushing may itself induce other experimental artefacts, for example by altering the grain-size distribution. Hence a consistent preparation and storage protocol needs to be adopted for any suite of experiments utilising synthetic ferrihydrite. Larsen and Postma (2001) and Cornell and Schwertmann (2003) point out that variations may also occur between ferrihydrites prepared in the same way but in different batches. Differences in de-watering and storage conditions between different laboratories may also produce labile Fe results that are not comparable.

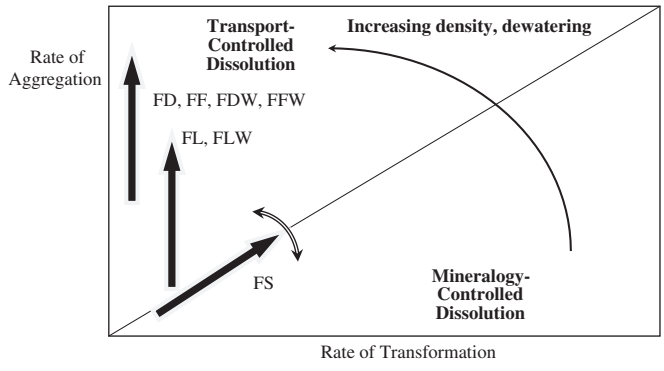

Fig. 8. Schematic representation of the effects of rate of aggregation and rate of transformation on the dissolution kinetics of ferrihydrites stored and treated in different ways. Arrows only show approximate positions of samples.

The ascorbic acid extraction is highly selective for the Fe present in fresh ferrihydrite (and the labile Fe present in ferrihydrites that have aggregated with age or de-watering) as compared to other common Fe-bearing minerals that may be present in atmospheric dust and glacial sediments. Aggregation also occurs in natural systems but only the most labile fraction of Fe is extracted by ascorbic acid from natural samples and only this fraction is potentially bioavailable unless aggregates can be broken down, for example by turbulence or abrasion. Unfortunately our data show that aggregation is produced by de-watering and sample collection and sample treatments need to minimize aggregation as far as possible. Ideally samples should be collected, stored and extracted wet, with the water content determined on a separate sample or, less satisfactorily, samples should be filtered, air-dried and stored by refrigeration. Freeze-drying and freezing should be avoided. We conclude that the labile fraction of Fe in ferrihydrite that is extracted by ascorbic acid provides a rough measure of the Fe that is, directly or indirectly, bioavailable.

Acknowledgements

Rob Raiswell thanks the Leverhulme Trust for the provision of an Emeritus Fellowship which provided funding for this work. LGB acknowledges support from the UK Natural Environment Research Council 'Weathering Science Consortium' NE/C004566/1. Andy Brown from LEMAS helped with the TEM work. The reviewers are thanked for their helpful comments.

Appendix A. Supplementary data

Supplementary data to this article can be found online at doi:10.1016/j.chemgeo.2010.09.002.

References

Banwart, S., Davies, S., Stumm, W., 1989. The role of oxalate in accelerating the dissolution of hematite (α-Fe_2O_3) by ascorbate. Colloids and Surfaces 39, 303–309.
Barbeau, K., Moffett, J.W., Caron, D.A., Croot, P.L., Erdner, D.L., 1996. Role of protozoan grazing in relieving iron limitations of plankton. Nature 380, 61–64.
Benning, L.G., Wilkin, R.T., Barner, H.L., 2000. Reaction pathways in the FeS system below 100 °C. Chemical Geology 167, 25–51.
Berger, C.J., Lippiat, S.M., Lawrence, M.G., Bruland, K., 2008. Application of a chemical leach technique for estimating labile particulate aluminium, iron and manganese in the Columbia River plume and coastal waters off Oregon and Washington. Journal of Geophysical Research 1113. doi:10.1029/2007JC004703.
Bottero, J.V., Arnaud, M., Villieras, F., Michot, L.J., Dedonato, P., Francois, M., 1993. Journal of Colloid and Interface Science 159, 43–52.
Brinza, L. 2010. Interaction of Mo and V with Iron Nanoparticles. University of Leeds, Ph. D thesis.
Canfield, D.E., 1989. Reactive iron in marine sediments. Geochimica et Cosmochimica Acta 53, 619–632.
Chen, Y., Siefert, R.L., 2003. Determination of various types of labile atmospheric iron over remote oceans. Journal of Geophysical Research 108. doi:10.1029/2003JD003515.
Chester, R., Hughes, M.J., 1967. A chemical technique for the separation of ferromanganese minerals, carbonate minerals and adsorbed trace elements for pelagic sediments. Chemical Geology 2, 249–262.
Christoffersen, J., Christoffersen, M.R., 1976. The kinetics of dissolution of calcium sulphate dihydrate in water. Journal of Crystal Growth 35, 79–88.
Christoffersen, J., Christoffersen, M.R., Kjaergaard, N., 1978. The kinetics of dissolution of calcium hydroxyapatite in water at constant pH. Journal of Crystal Growth 43, 501–511.
Cornell, R.M., Schwertmann, U., 2003. The Iron Oxides. Wiley, New York. 703p.
Cwiertny, D.W., Handler, R.M., Schaefer, M.V., Grassian, V.H., Scherer, M.M., 2009. Interpreting nanoscale size-effects in aggregated Fe-oxide suspensions: reaction of Fe(II) with goethite. Geochimica et Cosmochimica Acta 72, 1365–1380.
Davidson, L.E., Shaw, S., Benning, L.G., 2008. The kinetics and mechanisms of schwertmannite transformation to goethite and hematite under alkaline conditions. American Mineralogist 93, 1326–1337.
Deng, Y., Stumm, W., 1994. Reactivity of iron (III) oxyhydroxides—implications for redox cyclng of iron in natural waters. Applied Geochemistry 9, 23–26.
Dos Santos, M., Morando, P.J., Blesa, M.A., Banwart, S., Stumm, W., 1990. The reductive dissolution of iron oxides by ascorbate. Journal of Colloid and Interface Science 138, 74–82.
Ferdelman, T.G., 1988. The distribution of sulphur, iron, manganese, copper and uranium in a salt marsh sediment core as determined by a sequential extraction method. University of Delaware, MS thesis.

Gilbert, B., Lu, G., Kim, C.S., 2007. Stable cluster formation in aqueous suspensions of iron oxyhydroxide nanoparticles. Journal of Colloid and Interface Science 313, 152–159.
Gilbert, B., Ono, R.K., Ching, K.A., Kim, C.S., 2009. The effects of nanoparticle aggregation processes on aggregate structure and metal uptake. Journal of Colloid and Interface Science 339, 285–295.
Hyacinthe, C., Van Cappellen, P., 2004. An authigenic iron phosphate phase in estuarine sediments: composition, formation and chemical reactivity. Marine Chemistry 91, 227–251.
Hyacinthe, C., Bonneville, S., Van Cappellen, P., 2006. Reactive iron (III) in sediments: chemical versus microbial extractions. Geochimica et Cosmochimica Acta 70, 4166–4180.
Janney, D.E., Cowley, J.M., Buseck, P., 2000. Structure of synthetic 2-line ferrihydrite by electron nanodiffraction. American Mineralogist 85, 1180–1187.
Janney, D.E., Cowley, J.M., Buseck, P., 2001. Structure of 6-line ferrihydrite by electron nanodiffraction. American Mineralogist 86, 327–335.
Johnson, K.S., Coale, K.H., Elrod, V.A., Tindale, N.W., 1994. Iron photochemistry in seawater from the equatorial Pacific. Marine Chemistry 46, 319–334.
Kostka, J.E., Luther III, G.W., 1994. Partitioning and speciation of solid phase iron in saltmarsh sediments. Geochimica et Cosmochimica Acta 58, 1701–1710.
Larsen, O., Postma, D., 2001. Kinetics of reductive dissolution of lepidocrocite, ferrihydrite, and goethite. Geochimica et Cosmochimica Acta 65, 1367–1379.
Liang, L., Hofmann, A., Gu, B., 2000. Ligand-induced dissolution and release of ferrihydrite colloids. Geochimica et Cosmochimica Acta 64, 2027–2037.
Liu, X., Millero, F.J., 2002. The solubility of iron in seawater. Marine Chemistry 77, 43–54.
Logan, B.E., Kilps, J.R., 1995. Fractal dimensions of aggregates formed in different fluid mechanical environments. Water Research 29, 443–453.
McKeague, J.A., Day, J.H., 1966. Dithionite- and oxalate-extractable Fe and Al as aids in differentiating various classes of soils. Canadian Journal of Soil Science 46, 13–22.
Mehra, O.P., Jackson, M.L., 1960. Iron oxide removal from soils and clays by a dithionite–citrate system buffered with sodium carbonate. Clays and Clay Minerals 7, 317–327.
Moffett, J.W., 2001. Transformation among different forms of iron in the ocean. In: Turner, D.R., Hunter, K.A. (Eds.), The Biogeochemistry of Iron in Seawater. Wiley, New York, pp. 343–372.
Nodwell, L.M., Price, N.M., 2001. Direct use of inorganic colloidal iron by marine thixotrophic phytoplankton. Limnology and Oceanography 46, 765–777.
Nurmi, J.T., Tratnyek, P.G., Sarathy, V., Baer, D.R., Amonette, J.E., Pecher, K., Wang, C., Linehan, J.C., Matson, D.W., Penn, R., Driessson, M.D., 2005. Charaterization and properties of metallic iron nanoparticles: spectroscopy, electrochemistry and kinetics. Environmental Science and Technology 39, 1221–1230.
Philips, E.J.P., Lovely, D.R., 1987. Determination of Fe(II) and Fe(III) in oxalate extracts of sediment. Soil Science Society of America Journal 51, 938–941.
Postma, D., 1993. The reactivity of iron oxides in sediments: a kinetic approach. Geochimica et Cosmochimica Acta 57, 5027–5034.
Poulton, S.W., Canfield, D.E., 2005. Development of a sequential extraction procedure for iron: implications for iron partitioning in continentally derived particulates. Chemical Geology 214, 209–221.
Raiswell, R., Canfield, D.E., Berner, R.A., 1994. A comparison of iron extraction methods for the determination of degree of pyritization and recognition of iron-limited pyrite formation. Chemical Geology 111, 101–111.
Raiswell, R., Tranter, M., Benning, L.G., Siegert, M., De'ath, R., Huybrechts, P., Payne, T., 2006. Contributions from glacially derived sediment to the global iron (oxyhydr) oxide cycle: implications for iron delivery to the oceans. Geochimica et Cosmochimica Acta 70, 2765–2780.
Raiswell, R., Benning, L.G., Davidson, L., Tranter, M., 2008a. Nanoparticulate bioavailable iron minerals in icebergs and glaciers. Mineralogical Magazine 72, 345–348.
Raiswell, R., Benning, L.G., Tranter, M., Tulaczyk, S., 2008b. Bioavailable iron in the Southern Ocean: the significance of the iceberg conveyor belt. Geochemical Transactions 9. doi:10.1186/1467-4866-9-7.
Raiswell, R., Benning, L.G., Davidson, L., Tranter, M., Tulaczyk, S., 2009. Schwertmannite in wet, acid and oxic microenvironments beneath polar and polythermal glaciers. Geology 37, 431–434.
Reyes, J., Torrent, J., 1997. Citrate-ascorbate as a highly selective reactant for poorly crystalline iron oxides. Soil Science Society of America Journal 61, 1647–1654.
Rich, H.W., Morel, F.M.M., 1990. Availability of well-defined iron colloids to the marine diatom *Thalassiosira weissflogii*. Limnology and Oceanography 35, 652–662.
Rose, A.L., Waite, T.D., 2003. Kinetics of hydrolysis and precipitation of ferric iron in seawater. Environmental Science and Technology 37, 3897–3903.
Scheinost, A.C., Abend, S., Pandya, K.I., Sparks, D.L., 2001. Kinetic controls on Cu and Pb sorption by ferrihydrite. Environmental Science and Technology 35, 1090–1096.
Schwertmann, U., Stanjek, H., Becher, H.-H., 2004. Long-term in vitro transformation of 2-line ferrihydrite to goethite/hematite at 4, 10, 15 and 25 °C. Clay Minerals 39, 433–438.
Shi, Z., Krom, M.D., Bonneville, S., Baker, A.R., Jickells, T.D., Benning, L.G., 2009. Formation of iron nanoparticles and increase in iron reactivity in mineral dust during simulated cloud processing. Environmental Science and Technology 43, 6592–6596.
Shi, Z., Krom, M.D., Bonneville, S., Baker, A.R., Bristow, C., Mann, G., Carslaw, K., McQuaid, J.B., Jickells, T., Benning, L.G., in press. Influence of chemical weathering and aging of iron oxides on the potential iron solubility of Saharan dust during simulated atmospheric processing. Global Biogeochemical Cycles.
Stanjek, H., Weidler, P.G., 1992. The effect of dry heating on the chemistry, surface area and oxalate solubility of synthetic 2-line and 6-line ferrihydrite. Clay Minerals 27, 397–412.
Sulzberger, B., Suter, D., Siffert, C., Banwart, S., Stumm, W., 1989. Dissolution of Fe(III) (hydr)oxides in natural waters: laboratory assessment on the kinetics controlled by surface coordination. Marine Chemistry 28, 127–144.
Visser, F., Gerringa, L.J.A., Van der Gaast, S.J., de Baar, H.J.W., Timmermans, K.R., 2003. The role of reactivity and content of iron of aerosol dust on growth rates of two Antarctic diatom species. Journal of Phycology 39, 1085–1104.
Waychunas, G., 2001. Structure, aggregation and characterization of nanoparticles. In: Banfield, J.F., Navrotsky, A. (Eds.), Nanoparticles and the Environment: Reviews in Mineralogy and Geochemistry, 44, pp. 105–166.
Wells, M.L., Mayer, L.M., 1991. The photoconversion of colloidal iron oxyhydroxides in seawater. Deep-Sea Research 38, 1379–1395.
Wells, M.L., Zorkin, N.G., Lewis, A.G., 1983. The role of colloid chemistry in providing a source of iron to phytoplankton. Journal of Marine Research 41, 731–746.
Wells, M.L., Mayer, L.M., Guillard, R.R.L., 1991. A chemical method for estimating the availability of iron tophytoplankton in seawater. Marine Chemistry 33, 23–40.
Yoshida, T., Hayash, K., Ohmoto, H., 2002. Dissolution of iron hydroxides by marine bacterial siderophore. Chemical Geology 184, 1–9.